

Computational Analysis on Longitudinal Equivalent Bending Stiffness under the Influence of Shield-tunnel Transverse Deformation

Ming-Yu LI^{1,a,*}, Zhang-Jun HUANG^{2,b}, Yan-Wei ZHANG^{1,c}, Xiao-Fei BIAN^{1,d}

¹Zhengzhou University, Henan Zhengzhou, 450001, China

²ERCHU CO., LTD. of China Railway Tunnel Group, Hebei Sanhe, 065200, China

^awudizhenjime@126.com, ^b812409787@qq.com, ^c347005051@qq.com, ^d1170005760@qq.com

*Corresponding author

Keywords: Shield Tunnel, Convergence Deformation, Longitudinal Equivalent Bending Stiffness, Elliptic Equation.

Abstract. In order to study the lining longitudinal deformation rule under the influence of the lining transverse deformation in the process of long-term settlement of operating metro shield tunnel with straight joint, based on the field test monitoring data of Tibet Road-Zhongxing Road shield tunnel in the M8 of Shanghai, and considering the tunnel convergence, this problem is studied by amending equivalent continuous model. Then there is a comparison between the existing theoretical methods and this calculation method. The results showed that, in the ring joints, no considering shearing, the maximum of ring joint open, the tension and compression stress of segment, and bolt stress slightly decrease with the increase of deformation of tunnel convergence under the bending. The smaller the curvature radius of the shield-tunnel longitudinal deformation is, the larger the ring joint open under the influence of tunnel convergence is.

Introduction

Due to the joint, the stiffness of the lining is reduced in the shield tunnel with straight joint. When the longitudinal differential settlement occurs, there is joint staggering and joint opening between the rings. These will cause the joint leakage, the segment crack and track irregularity, etc. endangering the safety of operational tunnel. Therefore, to ensure the safety of operational tunnel, it is very important of the deformation and force characteristics of the ring joint longitudinally along tunnel. But so far, this research is still at a preliminary stage. In the process of long-term settlement of operational tunnel, the transverse deformation and the longitudinal deformation often occur simultaneously with the longitudinal differential settlement increasing. For the reason, the influence of tunnel convergence should be considered when analyzing the longitudinal deformation and stress of the ring with straight joint. The longitudinal equivalent bending stiffness model was studied in the references[1, 2, 3, 4], but without having considered the relationship between the transverse deformation and the longitudinal deformation. To sum up, with considering the relationship between the transverse deformation and the longitudinal deformation, a new longitudinal equivalent bending stiffness model is put forward for interpreting the longitudinal deformation and force of shield tunnel with straight joint more accurately, and providing more valuable theoretical reference for the operational safety judgement of metro tunnel.

Field Measurement Test

Summary

The Tibet road ~ Zhongxing Road Tunnel of Shanghai metro line No.8 is 1226m. It is mainly through Gray muddy clay and Gray clay. The joint segment is used in the shield tunnel. Each lining ring contains a key block, two adjacent blocks, two standard blocks, and an arch bottom block. The design strength grade of segment concrete is C55. The joint bolt is M30. The elastic gasket used for joint waterproofing is composed of water swelling rubber and EPDM. The main design parameters are shown in table 1.

Tab.1 The Main Design Parameters

The segment	Value	The bolt	Value
Thickness(m)	0.35	diameter(m)	0.03
Width(m)	1	The number of Ring-joint bolts	17
Outer diameter (m)	6.2	The number of Longitudinal-joint bolts	12
Inner diameter (m)	5.5	The tensile yield strength (MPa)	640
Ring-joint initial deformation (m)	0	The elastic modulus of bolt (GPa)	206
The design value of the concrete compressive strength (MPa)	26	length(m)	0.4
The design value of the concrete tensile strength (MPa)	21		
The elastic modulus of concrete (MPa)	35500		

The field measurement test section is near the work well, standard section, and the connected aisle respectively, as shown in figure 1. Monitoring projects include the tunnel convergence and the joint opening. Monitoring period is one year. The monitoring frequency is 3 months.

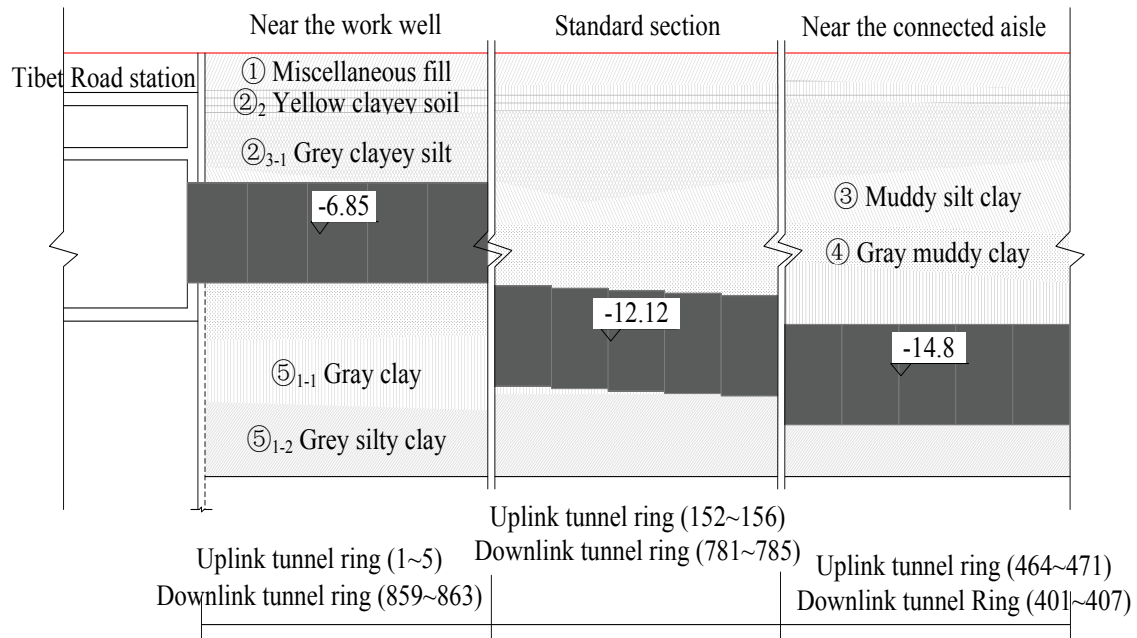


Fig. 1 Schematic Diagram of Monitoring

Tab. 2 Number of Points (tunnel convergence)

Monitoring area	Uplink tunnel		Downlink tunnel	
	Ring number	Point number	Ring number	Point number
Near the work well of Tibet Road	1	XZ1	863	XZ30
	2	XZ2	862	XZ29
	3	XZ3	861	XZ28
	4	XZ4	860	XZ27
	5	XZ5	859	XZ26
Standard section	152		785	
	153	XZ6	784	XZ25
	154	XZ7	783	XZ24
	155		782	
	156		781	
Near the connected aisle	464	XZ8	408	XZ23
	465	XZ9	407	XZ22
	466	XZ10	406	XZ21
	467	XZ11	405	XZ20
	468	XZ12	404	XZ19
	469	XZ13	403	XZ18
	470	XZ14	402	XZ17
	471	XZ15	401	XZ16

The initial coordinates is obtained by scanning fifty monitoring points on the ring with the total station. Then, fitting the initial coordinates gets the tunnel convergence by using for references[5,6,7,8,9]. The crack meter is used to survey the ring-joint opening between ring 783 and ring 784. One of crack meters is located in the key block, another is located in the standard block. The number of monitoring points is shown in table 2.

Data Analysis

With time increasing, the vertical compression deformation of tunnel increase gradually, as shown in figure 2.

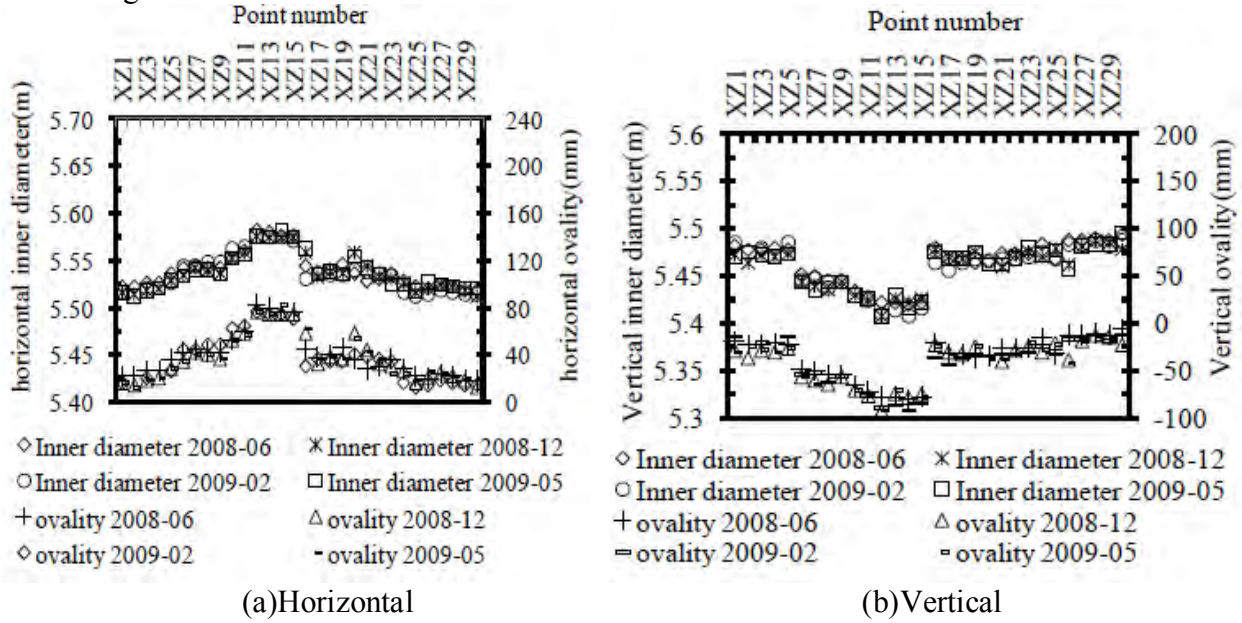


Fig.2 Distribution Curve of Tunnel Convergence

Because the tunnel convergence is constrained by the work well and the soil around the tunnel is reinforced when the shield machine got into or out of the work well, the tunnel convergence is relatively smaller near the work well. The soil around tunnel was disturbed in the tunneling press. Then with the connected aisle construction and the operating train vibration, the disturbed soil has been disturbed again. Compared to the other test section, the consolidation deformation of multiple disturbed soil is larger and the consolidation time is longer near the connected aisle. So that the tunnel convergence is relatively larger near here.

Correction Calculation of Longitudinal Equivalent Bending Stiffness

Model Calculation Assumes

According to the reference[2], the relative rotation will occur between the two adjacent linings. The relative angle is θ . In theory, the curvature is θ/l_s when the beam bending. The width of the segment is l_s . To solve the relationship of the bending moment and the curvature, the computational assumptions are as follows. The first is plane cross-section assumption. The lining ring is the homogeneous ring. On the cross section, the deformation of every point is proportional to the distance from the neutral axis. The second is not considering the joint staggering. The third, the bolt will bear all tension in the tension zone and the segment will bear all pressure in the compressive zone, when the relative rotation of the two adjacent linings appears in the joint. The fourth, to simplify the calculation, springs evenly distributed in the lining ring is instead of bolts.

$$K_r = \frac{E_b A_b}{2\pi l_b} \quad (1)$$

In the formula (1), the average line stiffness of the bolt is K_r (kN/m). The elastic modulus of the bolt is E_b (MPa). The cross-sectional area of the bolt is A_b (m²), $A_b = \pi d_b^2 / 4$. The diameter of the bolt is d_b (m). The length of the bolt is l_b (m). When the cross section in the elastic state, the stress of all bolts is less than P_y . The pretightening force of the bolt is P_y . The analysis of unit stress and strain is shown in figure 3. The relationship between the moment and curvature of the calculating unit is obtained according to the deformation compatibility condition and force equilibrium relationship.

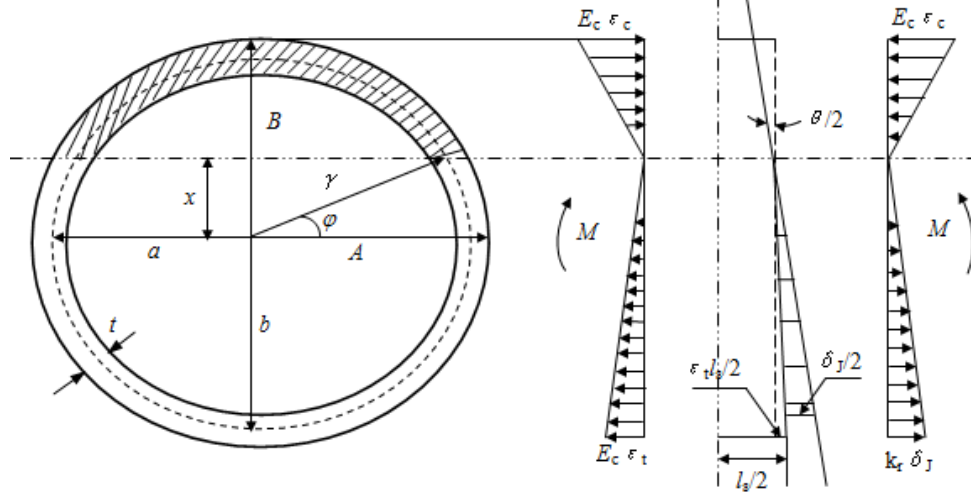


Fig.3 Diagram of Elastic Stress and Strain

Calculation Process

The deformation compatibility condition is as follows:

$$\varepsilon_c \frac{l_s}{2} = (B - x) \frac{\theta}{2} \quad (2)$$

$$\frac{b+x}{B+x} \varepsilon_t \frac{l_s}{2} + \frac{\delta_J}{2} = (b+x) \frac{\theta}{2} \quad (3)$$

In the formula (2) and formula (3), the semi-minor axis of elliptical lining ring is B (m), $B = b + t/2$. The long and short radius of elliptical lining ring respectively is a and b (m), $a = (t + d + \Delta_{DI})/2$, $b = (t + d + \Delta_{DV})/2$. The inner and outer diameter of the tunnel respectively is d and D (m). the vertical and horizontal convergence of the tunnel is Δ_{DI} and Δ_{DV} (mm), Δ_{DI} 、 $\Delta_{DV} > 0$. The maximum deformation of bolt is δ_J (mm). The width of the lining ring is t (m). The distance from the computing unit to the neutral axis is x (m). φ is the angle between the straight line of the computing unit and the neutral axis. $\varphi = \sin^{-1}(x/r)$. The tensile and compressive strain of the segment respectively is ε_t and ε_c .

The force equilibrium relationship is as follows:

$$2 \frac{E_c \varepsilon_c}{B-x} \int_{\varphi}^{\pi/2} (r \sin \alpha - x) r t d\alpha = 2 \frac{E_c \varepsilon_t}{B+x} \int_{-\pi/2}^{\varphi} (-r \sin \alpha + x) r t d\alpha = 2 \frac{K_r \delta_J}{b+x} \int_{-\pi/2}^{\varphi} (-r \sin \alpha + x) r d\alpha \quad (4)$$

$$2 \frac{E_c \varepsilon_c}{B-x} \int_{\varphi}^{\pi/2} (r \sin \alpha - x)^2 r t d\alpha + 2 \frac{E_c \varepsilon_t}{B+x} \int_{-\pi/2}^{\varphi} (-r \sin \alpha + x)^2 r t d\alpha = M \quad (5)$$

In the formula (4) and formula (5), The distance from the computing unit to the centroid is r (m), $r = b / \sqrt{1 - \varepsilon^2 \cos^2 \alpha}$. The elastic modulus of the segment is E_c (MPa); The ellipse center rate is ε , $\varepsilon = \sqrt{1 - b^2/a^2}$. The bending moment is M (kN·m).

The solution of simultaneous equations from the formula (1) to formula (5) is as follows:

$$\theta = \frac{Ml_s}{E_c t b^3 K} \quad (6)$$

$$K = \frac{\pi}{6} + \frac{\frac{\pi}{2} + \varphi}{3} \frac{8\sqrt{2} - 4\sqrt{2}\varepsilon^2 - 4\sqrt{2}\varepsilon^2 \sin \varphi - 6\sqrt{2}\varepsilon^2 \cos^2 \varphi}{(2 - \varepsilon^2 - \varepsilon^2 \sin \varphi)^{\frac{5}{2}}} + \frac{\frac{\pi}{2} - \varphi}{3} \frac{8\sqrt{2} - 4\sqrt{2}\varepsilon^2 + 4\sqrt{2}\varepsilon^2 \sin \varphi - 6\sqrt{2}\varepsilon^2 \cos^2 \varphi}{(2 - \varepsilon^2 + \varepsilon^2 \sin \varphi)^{\frac{5}{2}}} + \frac{\pi}{6} \frac{1 - \varepsilon^2 \cos^2 \varphi - 3\varepsilon^2 \sin^2 \varphi \cos^2 \varphi}{(1 - \varepsilon^2 \cos^2 \varphi)^{\frac{5}{2}}} - \frac{\sin \varphi}{\sqrt{1 - \varepsilon^2 \cos^2 \varphi}} \frac{\lambda}{\beta} \left(\frac{\sin \varphi}{\varepsilon \sqrt{1 - \varepsilon^2 \cos^2 \varphi}} \ln \frac{1 + \varepsilon \cos \varphi}{1 - \varepsilon \cos \varphi} + \frac{\frac{\pi}{2} + \varphi}{6} \left(\frac{1 - 3\varepsilon^2 \cos^2 \varphi + 2\varepsilon^2 \cos^4 \varphi}{(1 - \varepsilon^2 \cos^2 \varphi)^{\frac{5}{2}}} \right. \right. \\ \left. \left. + 8\sqrt{2} \frac{2 - \varepsilon^2 - \varepsilon^2 \sin \varphi - \varepsilon^2 \cos^2 \varphi}{(2 - \varepsilon^2 - \varepsilon^2 \sin \varphi)^{\frac{5}{2}}} + 1 \right) - \frac{\sin \varphi \cos \varphi}{(1 - \varepsilon^2 \cos^2 \varphi)^{\frac{3}{2}}} \right) ; \\ \lambda = \frac{\pi}{3} \left(1 + \frac{1}{\sqrt{1 - \varepsilon^2 \cos^2 \varphi}} \right) + \frac{4\sqrt{2}}{3} \left(\frac{\frac{\pi}{2} - \varphi}{\sqrt{2 - \varepsilon^2 + \varepsilon^2 \sin \varphi}} + \frac{\frac{\pi}{2} + \varphi}{\sqrt{2 - \varepsilon^2 - \varepsilon^2 \sin \varphi}} \right) ; \\ \beta = \frac{1}{\varepsilon} \ln \frac{1 + \varepsilon \cos \varphi}{1 - \varepsilon \cos \varphi} + \frac{\pi/2 + \varphi}{3} \frac{\sin \varphi}{\sqrt{1 - \varepsilon^2 \cos^2 \varphi}} \left(1 + \frac{4\sqrt{2}}{\sqrt{2 - \varepsilon^2 - \varepsilon^2 \sin \varphi}} + \frac{1}{\sqrt{1 - \varepsilon^2 \cos^2 \varphi}} \right) .$$

With the equivalent continuous beam bending, The formula of angle θ_{eq} is as follows:

$$\theta_{eq} = \frac{Ml_s}{(EI)_{eq}} \quad (7)$$

By comparing formula (6) with formula (7), the equivalent elastic bending rigidity of shield tunnel with straight joint $(EI)_{eq}$ is as follows:

$$(EI)_{eq} = E_c t b^3 K \quad (8)$$

The Elastic limit bending moment M_y (kN·m) of the unit is as follows:

$$\sigma_y = \frac{M_y}{(EI)_{eq}} b \left(\frac{\sin \varphi}{\sqrt{1 - \varepsilon^2 \cos^2 \varphi}} + 1 \right) = \frac{N_y}{(EA)_{eq}^T} \quad (9)$$

$$M_y = \frac{N_y (EI)_{eq}}{b \left(\frac{\sin \varphi}{\sqrt{1 - \varepsilon^2 \cos^2 \varphi}} + 1 \right) (EA)_{eq}^T} \quad (10)$$

The solution of simultaneous equations from the formula (2) to formula (6) is as follows:

$$\zeta E_s \frac{\pi d_b^2}{4 l_b} = \frac{E_c t}{n l_s} \frac{\frac{\pi}{3} a (1 + 4 \sqrt{1 - \frac{\varepsilon^2}{2}} + \sqrt{1 - \varepsilon^2})}{\beta / \eta - 1} \quad (11)$$

$$\text{In the formula (11), } \eta = \frac{1}{\varepsilon} \ln \frac{1 + \varepsilon \cos \varphi}{1 - \varepsilon \cos \varphi} - \frac{\pi/2 - \varphi}{3} \frac{\sin \varphi}{\sqrt{1 - \varepsilon^2 \cos^2 \varphi}} \left(1 + \frac{4\sqrt{2}}{\sqrt{2 - \varepsilon^2 + \varepsilon^2 \sin \varphi}} + \frac{1}{\sqrt{1 - \varepsilon^2 \cos^2 \varphi}} \right) .$$

The maximum compressive stress of the segment σ_c (MPa) is as follows:

$$\sigma_c = \frac{E_c}{\rho} \left(b + \frac{t}{2} - \frac{b \sin \varphi}{\sqrt{1 - \varepsilon^2 \cos^2 \varphi}} \right) \quad (12)$$

The maximum tensile stress of the bolt σ_t (MPa) is as follows:

$$\sigma_t = \frac{E_c}{\rho} \left(1 - \frac{\sin \varphi}{\sqrt{1 - \varepsilon^2 \cos^2 \varphi}} \frac{\lambda}{\beta} \right) \left(b + \frac{t}{2} + \frac{b \sin \varphi}{\sqrt{1 - \varepsilon^2 \cos^2 \varphi}} \right) \quad (13)$$

The maximum tensile stress of the bolt f_T (kPa) is as follows:

$$f_T = \zeta E_s \frac{l_s}{\rho l_b} \frac{\sin \varphi}{\sqrt{1 - \varepsilon^2 \cos^2 \varphi}} \frac{\lambda}{\beta} \left(b + \frac{b \sin \varphi}{\sqrt{1 - \varepsilon^2 \cos^2 \varphi}} \right) \quad (14)$$

The maximum opening of the joint δ_T is as follows:

$$\delta_T = \delta_J + \delta_0 = \frac{l_s}{\rho} \frac{\sin \varphi}{\sqrt{1 - \varepsilon^2 \cos^2 \varphi}} \frac{\lambda}{\beta} \left(b + \frac{b \sin \varphi}{\sqrt{1 - \varepsilon^2 \cos^2 \varphi}} \right) + \delta_0 \quad (15)$$

In the above formula, the curvature radius is ρ (m). The initial joint opening of the ring is δ_0 (mm). It is caused by assembling the segment in the process of construction. ζ is the reduction coefficient of the elastic modulus of the bolt sheared in the bolt hole, $0 < \zeta < 1$.

Example Analysis

In field test, the minimum longitudinal deformation curvature radius of the tunnel is ρ_{\min} , $\rho_{\min} = 3.33 \times 105\text{m}$. Axial tensile deformation is 0.079mm . $\delta_0 = 0$, $\zeta = 1$. For the ring-joint opening, the monitoring data and calculation results are compared in table 3. The comparison results is almost the same. It shows that the calculation method can reflect accurately the longitudinal deformation characteristic of shield tunnel with the straight joint.

Tab. 3 Comparative Analysis of the Ring-joint Opening

	Key block	Standard block	Arch bottom block
Field measurement test (mm)	0.079	0.096	0.101
This method (mm)	0.079	0.086	0.097

Parameter Analysis

Analyzed parameters include the tunnel convergence, the curvature radius, the tensile and compressive stress of the segment, the tensile stress, and the ring-joint opening, as shown from figure 4 to figure 7. For the pure bending tunnel, the ring-joint opening and the internal force of the segment and the bolt slightly reduce with the increase of the tunnel convergence. When the longitudinal curvature radius of the tunnel is small, the tunnel convergence has an obvious effect on the internal force of the segment and the bolt.

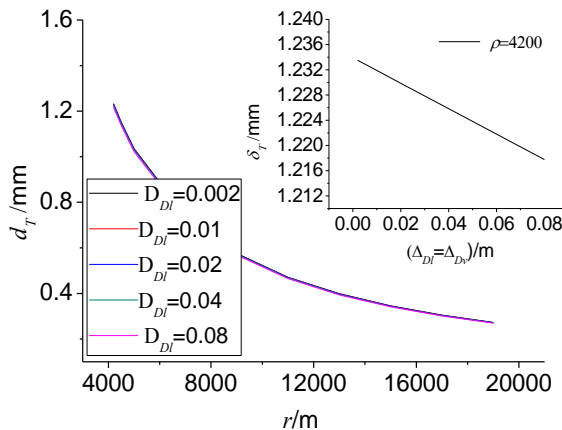


Fig.4 The Curve of Ring Joint Open and Tunnel Convergence

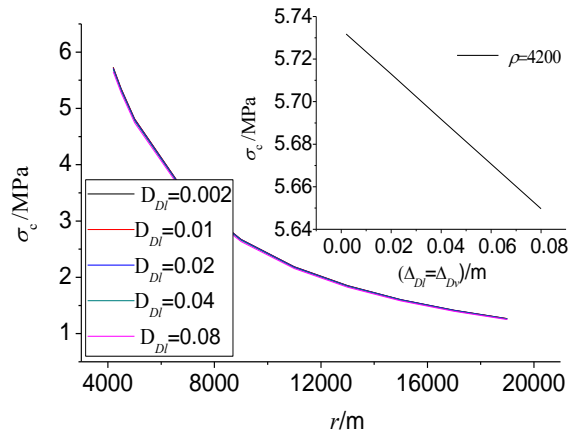


Fig.5 The Curve of Segment Stress and Tunnel Convergence

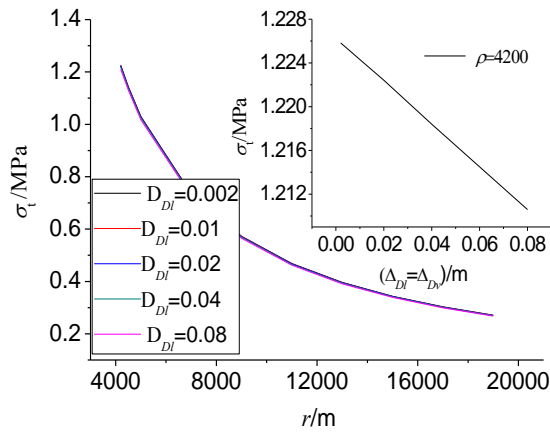


Fig. 6 The Curve of Segment Tensile Stress and Tunnel Convergence

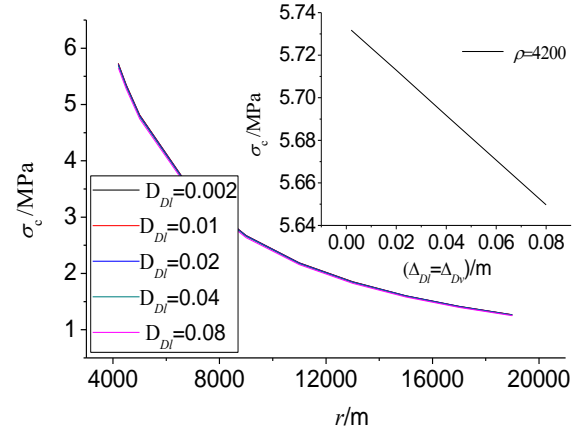


Fig. 7 The Curve of Longitudinal Tensile Stress in Bolts and Tunnel Convergence

Comparison and Analysis

In the analysis and calculation, according to the code for construction and acceptance of shield tunnel (GB50446-2008), $\rho_{\min}=15000\text{m}$, $f_T=6.4\times 10^5\text{kPa}$, $\Delta_{DI}=\Delta_{DV}=31\text{mm}$, $\delta_0=0$, $\zeta=1$. Comparing this method with the method of references[2,3,4], the analysis result is as shown in table 4.

When the longitudinal curvature of the shielded tunnel with the straight joint is the same, the comparative analysis of the ring-joint opening: the reference[4] < this article < the reference[3] < the reference[2]; the comparative analysis of the tensile stress of the bolt: this article < the reference[3] < the reference[2] < the reference[4].

When the maximum tensile stress of the bolt is the same, the comparative analysis of the ring-joint opening: the reference[4] < the reference[3] < this article < the reference[2]; the comparative analysis of the longitudinal curvature of the tunnel: the reference[2] < this article < the reference[3] < the reference[4].

Tab. 4 Comparison Table

Acceptance criteria	Differential calculation methods	δT (mm)	fT (105kPa)
$\rho_{\min}=15000\text{m}$	This method	0.34	1.77
	Reference[2]	0.4	3.84
	Reference[3]	0.35	2.48
	Reference[4]	0.32	3.97
Acceptance criteria	Differential calculation methods	ρ (m)	δT (mm)
$fT=6.4\times 10^5\text{kPa}$	This method	4149	1.24
	Reference[2]	3193	2.06
	Reference[3]	4682	1.11
	Reference[4]	8694	0.55

Conclusion

With the relationship between the transverse deformation and the longitudinal deformation considered, the existing longitudinal equivalent bending stiffness model is amended in this article. Then, based on the field test monitoring data of Tibet Road-Zhongxing Road shield tunnel in the M8 of Shanghai, the analysis results of this method and the reference[2,3,4] is compared. The main analysis conclusion is as follows:

For the pure bending tunnel, the ring-joint opening and the internal force of the segment and the bolt slightly reduce with the increase of the tunnel convergence. When the longitudinal

curvature radius of the tunnel is small, the tunnel convergence has an obvious effect on the internal force of the segment and the bolt.

In the process of long-term settlement of operational tunnel, the transverse deformation and the longitudinal deformation often occur simultaneously with the longitudinal differential settlement increasing. In this article, the deformation and force of the ring joint is only analyzed under the pure bending state. The longitudinal equivalent stiffness model of the shear and tension should be studied in the future research.

References

- [1]Y.G. Lin, S.M. Liao, G.B. Liu, A discussion of the factors effecting on longitudinal deformation of subway tunnel, *Underground Space*. Vol. 20 (2000) No.4, pp. 264-267. (In Chinese)
- [2]Y.D. Ye, Research on deformation and method of health diagnose of operational subway structures in soft soil. (Ph.D., Tongji University, China 2007). (In Chinese)
- [3]Y.L. Zheng, W. X. Han, Q.H. Tong, etc., Study on longitudinal crack of shield tunnel segment joint due to asymmetric settlement in soft soil, *Chinese journal of rock mechanics and engineering*. Vol. 24 (2005) No.24, pp. 4552-4558. (In Chinese)
- [4]Z.P. Lu, The safety evaluation research of metro shield tunnel during construction and operation based on static measured data. (Ph.D., Tongji University, China 2008). (In Chinese)
- [5]C. Yan, The application of total station in tunnel deformation monitoring. (MS., Tongji University, China 2005). (In Chinese)
- [6]W.S.Qiu, *Analytic geometry*, Peking University press, Beijing, 1999. (In Chinese)
- [7]P.L. Rosin, A note on the least squares fitting of ellipses, *Pattern recognition letters*. (1993) No.14, pp. 799-808.
- [8]W. Gander, G.H. Golub, R. Strebler, Least-Square fitting of circles and ellipses, *BIT*. (1994) No.43, pp. 558-578.
- [9]G. Taubin, Estimation of planar curves, surfaces and nonplanar space curves defined by implicit equations with applications to edge and range image segmentation, *IEEE trans pattern analysis and machine intelligence*. Vol.13, (1991) No.1, pp.1115-1138.